Available online at www.sciencedirect.com
ScienceDirect
Journal of Environmental Sciences 20(2008) 278–284
JOURNAL OF ENVIRONMENTAL SCIENCES
ISSN 1001-0742
CN 11-2629/X
www.jesc.ac.cn

Three-dimensional eutrophication model and application to Taihu Lake, China

MAO Jingqiao[1], CHEN Qiuwen[1,*], CHEN Yongcan[2]

1. State Key Laboratory of Urban and Regional Ecology, Research Centre for Eco-Environmental Sciences, Chinese Academy of Sciences, Beijing 100085, China. E-mail: mao.jq@rcees.ac.cn
2. Department of Hydraulic Engineering, Tsinghua University, Beijing 100084, China

Received 6 April 2007; revised 30 October 2007; accepted 1 November 2007

Abstract

Taihu Lake, the largest freshwater shallow lake in eastern China, has suffered from severe eutrophication over the past two decades. This research developed a three-dimensional eutrophication model to investigate the eutrophication dynamics. The model fully coupled the biological processes and hydrodynamics, and also took into account the effects of sediment release and the external loads from the tributaries. After sensitivity analyses, the key parameters were defined and then calibrated by the field observation data. The calibrated model was applied to study the seasonal primary productions and its regional differences. The comparisons between model results and field data in year 2000 indicated that the model is able to simulate the eutrophication dynamics in Taihu Lake with a reasonable accuracy. From the simulation experiments, it was found that the meteorological forcing have significant influences on the temporal variations of the eutrophication dynamics. The wind-induced circulation and sediment distribution play an important role in the spatial distribution of the algae blooms.

Key words: eutrophication dynamics; algae bloom; sediment distribution; Taihu Lake

Introduction

Taihu Lake, situated in the Yangtze Delta, is the third largest lake in China, with a surface area of 2,338 km^2 and a total volume of 4.43×10^9 m^3. The lake has a drainage area of 36,500 km^2 and an average depth of 1.9 m. The mean hydraulic retention time is about 300 d. This lake contains four major embayment that are Zhushan Bay, Meiliang Bay, Gong Bay, and East Bay (Fig.1). There are 219 tributaries to the lake, whereas the discharges of most of them are very small. The maximum mean discharge of the tributary is 26.8 m^3/s. The water quality of this lake has seriously deteriorated and nuisance algae blooms often occur in the summer and early fall in most areas. The blooms are thought to be the result of a combination of high nutrient loads and weak hydrodynamics.

Because of the important role for water supply, recreation, fisheries, agriculture and irrigation, Taihu Lake has received extensive studies in the past two decades. Liang and Zhong (1994) developed a three-dimensional (3D) hydrodynamic model for the lake, which revealed that the circulation is primarily driven by wind. Most of hydrodynamic models for Taihu Lake were based on finite difference method and the σ-coordinates system (Hu *et al*., 1998; Pang *et al*., 1998). On the basis of the hydrodynamic models, water quality models have been initiated for the lake. However, due to the high complexity of aquatic ecosystem, these modules mainly focused on the spatial distribution of nutrients (nitrogen and phosphorus) and dissolved organics (Zhu and Cai, 1998; Hu and Qing, 2002; Hong, 2005). They are highly simplified, either ignoring the influence of current structure (Xu *et al*., 2001) or dividing the lake into finite segments to solve 1D hydrodynamic equation (Pang *et al*., 1998). As an alternative, a fuzzy logic model was developed (Chen and Mynett, 2003) through exploring the limited data and the available experts' knowledge.

Although the previous researches are able to identify the basic eutrophication status of Taihu Lake, they failed to provide enough information about temporal variations of the chemical and biological processes. Integration of ecological and hydrodynamic processes is certainly far from establishment for this case. In order to have insightful understandings to the detailed eutrophication features of Taihu Lake, this study developed a 3D model which coupled the physical and biochemical processes. The model was calibrated by the field observations and then applied to simulate the influences of sediment distribution and meteorological forcing on the spatial-temporal dynamics of the primary production in Taihu Lake.

1 Model framework

Similar to the existing eutrophication models (Muhammetoglu and Soyupak, 2000; Drago *et al*., 2001; Lonin and Tuchkovenko, 2001; Chau, 2004), the developed model

* Corresponding author. E-mail: qchen@rcees.ac.cn.

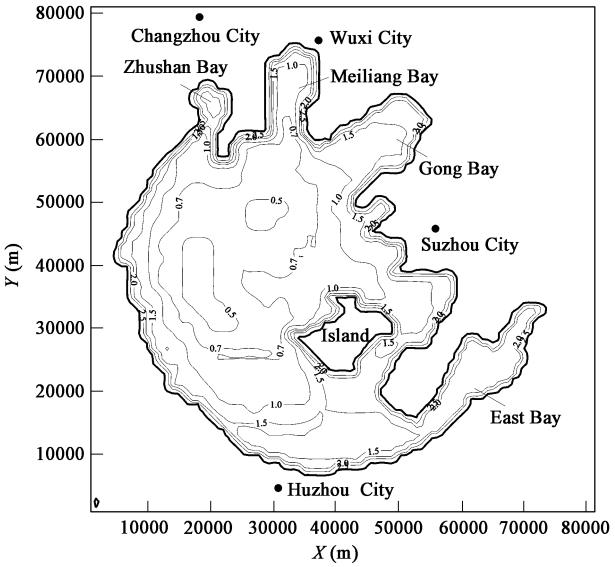

Fig. 1 Topographic overview of Taihu Lake (from Taihu Basin Authority).

consists of a hydrodynamic module and a biochemical module. Based on hydrodynamic simulations, the spatial-temporal variations of non-conservative chemical and biological substances can be simulated by solving a series of advection-diffusion equations.

1.1 Hydrodynamics

In shallow lakes, the vertical acceleration is small compared to gravity acceleration, so the momentum equation along vertical direction can be reduced to the hydrostatic law (Drago and Iovenitti, 2000). The integration of vertical processes in the presence of large variation of bathymetry using constant level thickness often introduces numerical errors. To deal with the high bottom slopes, the σ-coordinate was used through the coordinate transformation (Eq.(1)), which reproduces the bathymetry variations more accurately.

$$z' = \sigma = \frac{z+h}{\zeta+h} = \frac{z+h}{H} \qquad \sigma \in [0,1] \tag{1}$$

where, h is the depth from the mean water level (m), ζ is the water level (m), H is the total depth (m) and z is the distance from surface to specific point (m). Thus, σ ranges from 0 at the bottom to 1 at the surface.

The governing equations under σ-coordinates system are presented as follows:

$$\frac{\partial \zeta}{\partial t} + \frac{\partial Hu}{\partial x} + \frac{\partial Hv}{\partial y} + \frac{\partial w}{\partial \sigma} = 0 \tag{2}$$

$$\frac{\partial u}{\partial t} + u\frac{\partial u}{\partial x} + v\frac{\partial u}{\partial y} + w\frac{\partial u}{\partial \sigma} = fv - g\frac{\partial \zeta}{\partial x} + A_x\frac{\partial^2 u}{\partial x^2} + A_y\frac{\partial^2 u}{\partial y^2} + \frac{\gamma_i}{H^2}\frac{\partial^2 u}{\partial \sigma^2} \tag{3}$$

$$\frac{\partial v}{\partial t} + u\frac{\partial v}{\partial x} + v\frac{\partial v}{\partial y} + w\frac{\partial v}{\partial \sigma} = -fu - g\frac{\partial \zeta}{\partial y} + A_x\frac{\partial^2 v}{\partial x^2} + A_y\frac{\partial^2 v}{\partial y^2} + \frac{\gamma_i}{H^2}\frac{\partial^2 v}{\partial \sigma^2} \tag{4}$$

where, u, v, w are respectively x-, y-, σ-components of current (m/s), f is the Coriolis parameter, ρ is the water density (kg/m^3), P_a is the atmospheric pressure, A_x, A_y are the horizontal eddy viscosity coefficients (m^2/s), γ_i is the vertical eddy viscosity coefficient (m^2/s).

For completing the governing equations, continuity equation has to be integrated along the σ-direction to provide an additional equation:

$$\frac{\partial \zeta}{\partial t} + \int_0^1 \frac{\partial Hu}{\partial x} d\sigma + \int_0^1 \frac{\partial Hv}{\partial y} d\sigma = 0 \tag{5}$$

1.2 Biochemical processes

The interplay between the mass balance of multiple chemical elements and trophic dynamics are explicitly considered (Zhang *et al*., 2004). This model simulates the phytoplankton (C_1), nitrogen (C_2), phosphorus (C_3), zooplankton (C_4), detritus (C_5), dissolved organic matter (DOM, C_6), and dissolved oxygen (DO, C_7) as well as elemental cycles in sediment including nitrogen in sediment (C_8), phosphorus in sediment (C_9) and organic matter in sediment (C_{10}). The mass balance equation for a state variable is expressed as:

$$\frac{\partial C}{\partial t} = -\left(u\frac{\partial C}{\partial x} + v\frac{\partial C}{\partial y} + w\frac{1}{H}\frac{\partial C}{\partial \sigma}\right) + \left(D_x\frac{\partial^2 C}{\partial x^2} + D_y\frac{\partial^2 C}{\partial y^2} + \frac{D_\sigma}{H^2}\frac{\partial^2 C}{\partial \sigma^2}\right) + S + D \tag{6}$$

where, C is the concentration of a state variable (mg/L), D_x, D_y and D_σ are the diffusion coefficients (m^2/s) in x, y and σ directions, S is the source/sink term (loads of pollutant, suspended solids or plankton) and D is the reaction terms (Eqs.(7) and (11)–(19)).

The conceptual diagram for the ecosystem model is shown in Fig.2. Phytoplankton plays a central role in the carbon and nutrient cycles that comprise the model ecosystem. Phytoplankton growth is governed by the available nutrients such as dissolved inorganic nitrogen (DIN) and dissolved inorganic phosphorus (DIP) is represented by "R1" in Fig.2. Furthermore, the effects of light and temperature on phytoplankton growth are also included. DIN and DIP are returned from the phytoplankton metabolism (R2′) and zooplankton metabolism (R4′). During the decays, phytoplankton and zooplankton are decomposed into detritus with oxygen consumption (R2″, R3″ and R4″). Detritus is decomposed to DOM (R5), or settle to the sediment (R13). However, detritus can also be released from sediment (R10). DOM decomposition is the main resource of the nutrients concentration increase (R6). Release of DIN, DIP and DOM from sediment occurs in overlying water (R7, R8 and R9). Dissolved oxygen is consumed by phytoplankton respiration (R14), zooplankton respiration (R15), and decomposition of DOM (R17) in water or sediment (R11), whereas it also could be resumed by phytoplankton photosynthesis (R16) and atmospheric reaeration at the surface (R12).

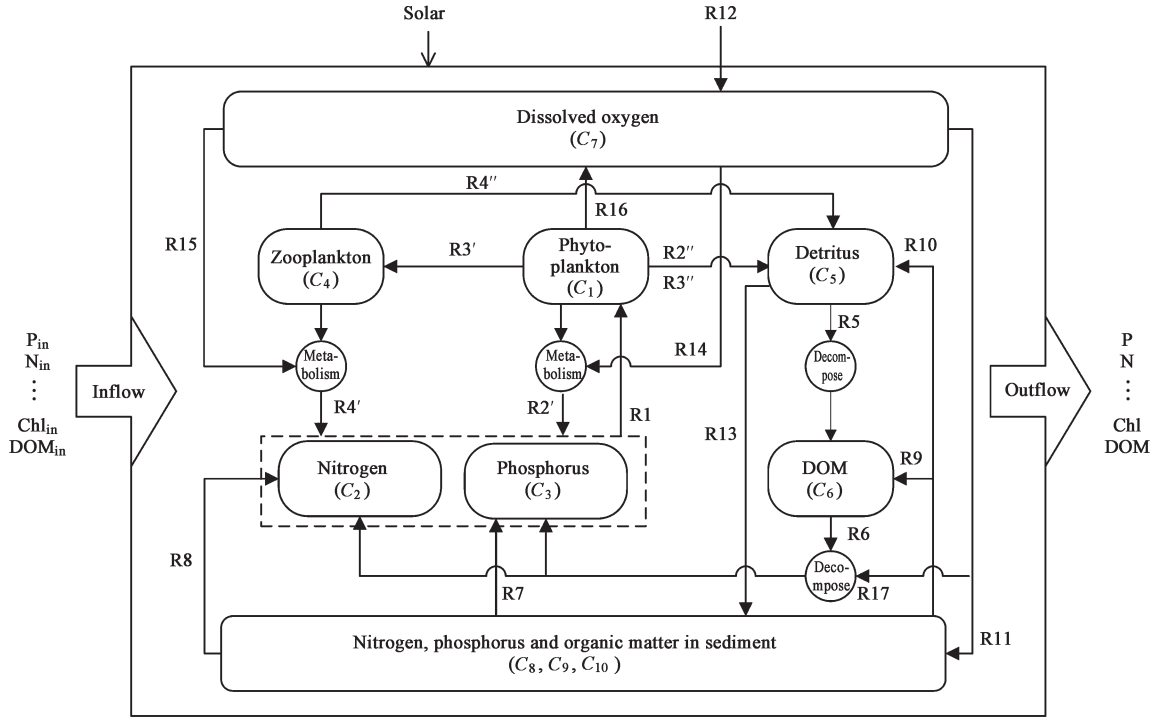

Fig. 2 Conceptual diagram of the biochemical module (each box represents a state variable and the arrows represent kinetic interactions among state variables).

Phytoplankton

The biochemical interaction term for phytoplankton considers phytoplankton production and losses due to basal metabolism and zooplankton grazing. Impacts of nutrients, light and water temperature on phytoplankton growth are included using a multiplicative model. In this study, chlorophyll concentration is used as the phytoplankton indicator.

$$D(C_1) = \mu_{\text{Chl-}a} \cdot f_{\text{T}} \cdot f_{\text{I}} \cdot f_{\text{NP}} \cdot C_1 - k_{d\text{Chl-}a}\theta_{\text{Chl-}a}^{(T-20)} \times \frac{C_7}{K_{\text{DO}} + C_7} C_1 - K_{\text{Zp}} \frac{C_1}{K_{m\text{Zp}} + C_1} C_4 \tag{7}$$

where, $\mu_{\text{Chl-}a}$ is the maximum phytoplankton growth rate (1/d); f_{T}, f_{I} and f_{NP} are the limitations due to temperature and light intensity and nutrients respectively, $\theta_{\text{Chl-}a}$ is the temperature constant, $k_{d\text{Chl-}a}$ is the phytoplankton mortality rate (1/d); K_{DO} is the DO consumption half saturation constant (mg/L), K_{Zp} is the zooplankton predation rate (1/d), $K_{m\text{Zp}}$ is the predation half saturation constant (mg/L).

The water temperature limitation factor f_{T} is calculated using an exponential or parabola expression (Zhang *et al.*, 2004); f_{NP} is calculated based on Michaelis-Menten equation and Liebig's law of the minimum; f_{I} is obtained by the Steele's equation (Muhammetoglu and Soyupak, 2000). These affecting functions are defined respectively by:

$$f_T = \theta_{\text{Chl-}a}^{(T-20)} \quad \text{or} \quad f_{\text{T}} = 1 - \left(T - T_{\text{opt}}\right)^2 \Big/ T_{\text{opt}}^2 \tag{8}$$

$$f_{\text{I}} = \frac{I \times \exp(-kh)}{I_s} \times \exp\left(1 - \frac{I \times \exp(-kh)}{I_s}\right) \tag{9}$$

$$f_{\text{NP}} = \min\left(\frac{C_2}{K_{m\text{N}} + C_2}, \frac{C_3}{K_{m\text{P}} + C_3}\right) \tag{10}$$

where, T_{opt} is the optimum water temperature (°C), I is the incident light intensity at water surface (MJ/(m^2·d)), I_{s} is the saturation light intensity (MJ/(m^2·d)), h is the water depth of the specified location (m), light attenuation is calculated by $k = \alpha + \beta C_1$ in which α is the water extinction coefficient and β is the phytoplankton extinction coefficient, $K_{m\text{N}}$ and $K_{m\text{P}}$ are the half saturation constant for nitrogen and phosphorus respectively (mg/L).

Nitrogen and phosphorus

$$\begin{aligned} D(C_2) = {} & -\gamma_{\text{NChl-}a}\mu_{\text{Chl-}a} \cdot f_{\text{T}} \cdot f_{\text{I}} \cdot f_{\text{NP}} \cdot C_1 \\ & + \gamma_{\text{NChl-}a}(1 - Y_{\text{Chl-}a}) k_{d\text{Chl-a}}\theta_{\text{Chl-}a}^{(T-20)} \frac{C_7}{K_{\text{DO}} + C_7} C_1 \\ & + \gamma_{\text{NZp}}\left(1 - Y_{\text{Zp}}\right) k_{d\text{Zp}}\theta_{\text{Zp}}^{(T-20)} \frac{C_7}{K_{\text{DO}} + C_7} C_4 \\ & + \gamma_{\text{NC}} k_{d\text{C}}\theta_{\text{DOM}}^{(T-20)} \frac{C_7}{K_{\text{DO}} + C_7} C_6 \end{aligned} \tag{11}$$

$$\begin{aligned} D(C_3) = {} & -\gamma_{\text{PChl-}a}\mu_{\text{Chl-}a} \cdot f_{\text{T}} \cdot f_{\text{I}} \cdot f_{\text{NP}} \cdot C_1 \\ & + \gamma_{\text{PChl-}a}(1 - Y_{\text{Chl-}a}) k_{d\text{Chl-a}}\theta_{\text{Chl-}a}^{(T-20)} \frac{C_7}{K_{\text{DO}} + C_7} C_1 \\ & + \gamma_{\text{PZp}}\left(1 - Y_{\text{Zp}}\right) K_{\text{Zp}} \frac{C_1}{K_{m\text{Zp}} + C_1} C_4 \\ & + \gamma_{\text{PC}} k_{d\text{C}}\theta_{\text{DOM}}^{(T-20)} \frac{C_7}{K_{\text{DO}} + C_7} C_6 \end{aligned} \tag{12}$$

where, $\gamma_{\text{NChl-}a}$ is the nitrogen-phytoplankton stoichiometric relation, γ_{NZp} is the nitrogen-zooplankton stoichiometric relation; γ_{NC} is the nitrogen-DOM stoichiometric relation, $\gamma_{\text{PChl-}a}$ is the phosphorus-phytoplankton stoichiometric relation, γ_{PZp} is the phosphorus-zooplankton stoichiometric relation, γ_{PC} is the phosphorus-DOM stoichiometric relation.

Eqs. (8) and (9) consider the local variation of nitrogen and phosphorus due to phytoplankton growth and respiration, zooplankton respiration and DOM decomposition.

Zooplankton

The growth and mortality of zooplankton are taken into account in Eq. (13):

$$D(C_4) = \gamma_{\mathrm{ZpChl}\text{-}a} Y_{\mathrm{ZpChl}\text{-}a} K_{\mathrm{Zp}} \frac{C_1}{K_{\mathrm{mZp}} + C_1} C_4 - k_{d\mathrm{Zp}} \theta_{\mathrm{Zp}}^{(T-20)} \frac{C_7}{K_{\mathrm{DO}} + C_7} C_4 \quad (13)$$

where, $\gamma_{\mathrm{ZpChl}\text{-}a}$ is the zooplankton-phytoplankton stoichiometric relation, $\gamma_{\mathrm{ZpChl}\text{-}a}$ is the predation efficiency factor, k_{dZp} is the zooplankton mortality rate (1/d), θ_{Zp} is the temperature constant.

Detritus

$$D(C_5) = \gamma_{\mathrm{DtChl}\text{-}a} Y_{\mathrm{Chl}\text{-}a} k_{d\mathrm{Chl}\text{-}a} \theta_{\mathrm{Chl}\text{-}a}^{(T-20)} \frac{C_7}{K_{\mathrm{DO}} + C_7} C_1 + \gamma_{\mathrm{DtChl}\text{-}a} \left(1 - Y_{\mathrm{ZpChl}\text{-}a}\right) K_{\mathrm{Zp}} \frac{C_1}{K_{m\mathrm{Zp}} + C_1} C_4 + Y_{\mathrm{zp}} R_4 - k_{d\mathrm{Dt}} \theta_{\mathrm{Dt}}^{(T-20)} C_5 - v_{\mathrm{sDt}} \frac{1}{H} \frac{\partial C_5}{\partial z} \quad (14)$$

where, $\gamma_{\mathrm{DtChl}\text{-}a}$ is the detritus-phytoplankton stoichiometric relation, $Y_{\mathrm{Chl}\text{-}a}$ is the respiration efficiency of phytoplankton, Y_{Zp} is the respiration efficiency of zooplankton, k_{dDt} is the decomposition rate of detritus (1/d), θ_{Dt} is the temperature constant, ν_{sDt} is the falling velocity of detritus (m/d).

DOM

$$D(C_6) = \gamma_{\mathrm{DOMDt}}\, k_{d\mathrm{Dt}} \theta_{\mathrm{Dt}}^{(T-20)} C_5 - k_{\mathrm{dc}} \theta_{\mathrm{DOM}}^{(T-20)} \frac{C_7}{K_{\mathrm{DO}} + C_7} C_6 \quad (15)$$

where, γ_{DOMDt} is the DOM-detritus stoichiometric relation, k_{dc} is the decomposition rate of DOM (1/d), θ_{DOM} is the temperature constant. Eq.(15) takes into account the local variation of DOM concentration due to the DOM released from detritus.

DO

$$D(C_7) = \gamma_{\mathrm{DoChl}\text{-}a} \mu_{\mathrm{Chl}\text{-}a} \cdot f_{\mathrm{T}} \cdot f_{\mathrm{I}} \cdot f_{\mathrm{NP}} \cdot C_1 - \gamma_{\mathrm{DoChl}\text{-}a} (1 - Y_{\mathrm{Chl}\text{-}a}) k_{d\mathrm{Chl}\text{-}a} \theta_{\mathrm{Chl}\text{-}a}^{(T-20)} \frac{C_7}{K_{\mathrm{DO}} + C_7} C_1 - \gamma_{\mathrm{DoZp}} \left(1 - Y_{\mathrm{Zp}}\right) k_{d\mathrm{Zp}} \theta_{\mathrm{Zp}}^{(T-20)} \frac{C_7}{K_{\mathrm{DO}} + C_7} C_4 - \gamma_{\mathrm{DOC}} k_{d\mathrm{C}} \theta_{\mathrm{DOM}}^{(T-20)} \frac{C_7}{K_{\mathrm{DO}} + C_7} C_6 \quad (16)$$

where, $\gamma_{\mathrm{DoChl}\text{-}a}$ is the DO-phytoplankton stoichiometric relation, γ_{DOZp} is the DO-zooplankton stoichiometric relation, γ_{DOC} is the DO-DOM stoichiometric relation.

Through the water surface, dissolved oxygen in the upper water is subtracted or added depending on the oxygen concentration contrasting with the saturation level. The exchange flux of DO through surface may be calculated by $k_{\mathrm{rDO}}(\mathrm{DO_{sat}}–C_7)/\Delta Z_n$, where $\mathrm{DO_{sat}}$ is the concentration of dissolved oxygen saturation (mg/L), ΔZ_n is the height of the surface layer (m). The exchange rate k_{rDO} is calculated depending on wind and temperature (Lonin and Tuchkovenko, 2001; Chau, 2004; Mao, 2005). Sedimentary oxygen demand is simply evaluated by $k_{\mathrm{DOS}}\theta_{\mathrm{DO}}{}^{(\mathrm{T}\text{-}20)}C_7$, where k_{DOS} is the oxygen consumption rate by sediment (1/d), and θ_{DO} is the temperature constant.

Sediment terms

Local variations of releasable nitrogen, phosphorus and organic matter in bottom sediment (Zhang *et al*., 2004), due to sedimentation of detritus and the release processes from sediment, are taken into account in this model.

$$\frac{\mathrm{d}C_8}{\mathrm{d}t} = \gamma_{\mathrm{ND}} k_{\mathrm{sed}} \frac{v_{\mathrm{sDt}} C_{5\mathrm{b}}}{H_{\mathrm{s}}} - \frac{H_{\mathrm{b}}}{H_{\mathrm{s}}} \frac{k_{sr\mathrm{Sn}}}{1000 H_{\mathrm{s}}} - \gamma_{\mathrm{ND}} \frac{H_{\mathrm{b}}}{H_{\mathrm{s}}} \frac{k_{sr\mathrm{Dt}}}{1000 H_{\mathrm{s}}} \quad (17)$$

$$\frac{\mathrm{d}C_9}{\mathrm{d}t} = \gamma_{\mathrm{PD}} k_{\mathrm{sed}} \frac{v_{\mathrm{sDt}} C_{5\mathrm{b}}}{H_{\mathrm{s}}} - \frac{H_{\mathrm{b}}}{H_{\mathrm{s}}} \frac{k_{sr\mathrm{Sp}}}{1000 H_{\mathrm{s}}} - \gamma_{\mathrm{PD}} \frac{H_{\mathrm{b}}}{H_{\mathrm{s}}} \frac{k_{sr\mathrm{Dt}}}{1000 H_{\mathrm{s}}} \quad (18)$$

$$\frac{\mathrm{d}C_{10}}{\mathrm{d}t} = \gamma_{\mathrm{CD}} k_{\mathrm{sed}} \frac{v_{\mathrm{sDt}} C_{5\mathrm{b}}}{H_{\mathrm{s}}} - \frac{H_{\mathrm{b}}}{H_{\mathrm{s}}} \frac{k_{sr\mathrm{Sc}}}{1000 H_{\mathrm{s}}} - \gamma_{\mathrm{CD}} \frac{H_{\mathrm{b}}}{H_{\mathrm{s}}} \frac{k_{sr\mathrm{Dt}}}{1000 H_{\mathrm{s}}} \quad (19)$$

where, k_{sed} is the fraction ration of sediment, $k_{sr\mathrm{Sn}}$, $k_{sr\mathrm{Sp}}$ and $k_{sr\mathrm{Sc}}$ are the release rate of nitrogen, phosphorus and organic matter respectively (mg/(m^2·d)), γ_{ND} is the nitrogen-sediment stoichiometric relation, $k_{sr\mathrm{Dt}}$ is the floatation rate of sediment (mg/(m^2·d)), H_{b} is the height of the overlying water layer (m), H_{s} is the sediment depth (m), γ_{PD} is the phosphorus-sediment stoichiometric relation, γ_{CD} is the organic matter-sediment stoichiometric relation, $C_{5\mathrm{b}}$ is the detritus concentration in the overlying water layer (mg/L).

1.3 Numerical method

The numerical solution of the governing equations uses a finite-difference spatial discretization, frontal-difference in temporal domain and central-difference in spatial domain, with a "C" grid staggering of the discrete variables. Water level and concentration of transported constituents are located at the center of the control volume, and the velocity components are located on the faces of the control volume. The wind stress on the water surface is formulized as $\tau_{\mathrm{w}x} = \rho_a \gamma_s W_x \sqrt{W_x^2 + W_y^2}$ or $\tau_{\mathrm{w}y} = \rho_{\mathrm{a}} \gamma_{\mathrm{s}} W_y \sqrt{W_x^2 + W_y^2}$ (Liang and Zhong, 1994), where ρ_{a} is the air density (1.25×10^{-3} g/cm^3), W_x and W_y are the wind speed components in x- and y-direction, respectively (m/s), γ_{DOC} is a coefficient calculated by the average wind speed at 10 meters over the surface: $\gamma_{\mathrm{s}} = 6.9 \times 10^{-3} + 7.5 \times 10^{-5} W$.

It is physically realistic to assume that the flow velocity close to the bottom has a logarithmic profile as a function of the distance from the wall. Introducing the parameter $\gamma_{\mathrm{b}} = (k/\ln(z/z_0))^2$, the bed shear stress may be presented by $\tau_{\mathrm{b}x} = \rho \gamma_{\mathrm{b}} u_{\mathrm{b}} \sqrt{u_{\mathrm{b}}^2 + v_{\mathrm{b}}^2}$ and $\tau_{\mathrm{b}y} = \rho \gamma_{\mathrm{b}} v_{\mathrm{b}} \sqrt{u_{\mathrm{b}}^2 + v_{\mathrm{b}}^2}$, where u is the current velocity at z distance from the wall, u* is the friction velocity; k is the Von Karman constant (0.4), z_0

is the rough height (0.002–0.01 m).

Flow fields, including water level, horizontal and vertical velocity components, and eddy viscosity parameters are computed by the hydrodynamic module and set as an input data file. The concentration distribution of water quality constituents in the water column can be obtained by solving mass transport equations numerically.

2 Simulation of Taihu Lake

2.1 Initial and boundary conditions

The computation domain of Taihu Lake was discretized by horizontal 1000×1000 m^2 cells and 3 equal-proportion vertical σ-layers. The hydrodynamic simulation time step was selected as 10 s, while biochemical simulation time step was enlarged to 90 s.

Taihu Lake is well known as a typical shallow lake with wind-driven current, mainly induced by varying wind field. For previous models, only prevailing southeast trade wind was considered as the forcing condition in summer to avoid potential numerical difficulties. In this study, a period of one year was selected for model simulation, so annual atmospheric data necessary for model simulation including wind speed and direction were collected from Wuxi City weather station (Fig.1), the closest comprehensive observation station for the lake.

Annual averages of external loads, including nutrients and DOM, from twenty-five tributaries (Fig.3) were collected. Because there is lack of specific phytoplankton, it was assumed that the chlorophyll-*a* concentrations are near to zero in the upstream river reaches, which is in accord with the real situation.

The field data of sediment thickness were collected and spatially interpolated for the computing grids, which then were used to evaluate the magnitude of release terms from sediment. The simple linear relationship between sediment thickness and flow velocity was assumed (Mao, 2005).

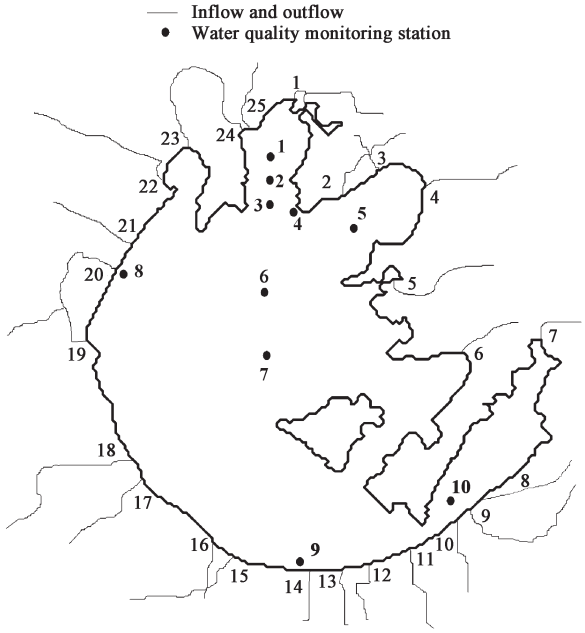

Fig. 3 Overview of inflow and outflow and water quality monitoring stations.

Firstly the calibrated model was spun up repeatedly using the forcing and boundary conditions of the period of December 1999. Using the output from the spin-up run as the initial condition, including flow currents and all water quality variables, the hindcast simulation was then performed for the next year (2000).

2.2 Sensitivity analysis and model calibration

Considering the large set of parameters involved in the biochemical module, it is difficult to calibrate them all. Therefore, a sensitivity analysis was performed by varying the values of parameters and analyzing the model outputs in the small semi-closed Wuli Bay, the heaviest polluted part of Meiliang Bay (Mao, 2005).

The basic steps of sensitivity analysis were: first, determining the ranges of parameter values according to the literature (Drago *et al*., 2001; Zhang *et al*., 2004; Mao, 2005); second, respectively inputting the maximum and minimum values of specified parameter into the scenario, with mean values specified for other parameters simultaneously; finally, assessing the performance of the specified parameter with the mean relative error:

$$\mathrm{MRE} = \left(\sum_{i=1}^{n} |P_{\max} - P_{\min}|\right) \Big/ n \tag{20}$$

where, n is the length of time series, $P_{\max}$ and $P_{\min}$ are the modeled maximum and minimum concentrations of phytoplankton.

Four most sensitive parameters, being listed in sequence according to MRE values ($k_{d\mathrm{Chl\text{-}a}}$ = 78.2%; $\mu_{\max}$ = 70.7%; T_{opt} = 67.8% and K_{Zp} = 59.5%), were selected to be primarily calibrated for the model. After calibration, the optimal values of calibrated parameters are: $k_{\mathrm{dChl\text{-}}a}$ = 0.27 (1/d), $\mu_{\max}$ = 1.28 (1/d), T_{opt} = 30 (°C) and K_{Zp} = 0.105 (1/d). Values of other parameters can be directly obtained from the literature, or be slightly calibrated, if necessary. The final parameter values are given in Table 1.

2.3 Results and discussion

The calibrated model was applied to simulate the eutrophication processes in the Taihu Lake during the year of 2000. Comparisons between modeled annual chlorophyll-*a* concentration and the field data at different stations are presented in Fig.4. Although there were some differences between measurement and simulation, trends and quantities of chlorophyll-*a* concentrations obtained from the model were generally in agreement with the observations.

Figures.4a and 4b show the simulated and observed values at the monitoring Stations 1 and 2 located in Meiliang Bay. It was found that there was a distinct phase delay between observed and computed at these two stations. According to the observation of 2000, algae blooms in Meiliang Bay occurred earlier than the other parts of this lake. Although at Station 2 the modeled maximum concentration agreed well with observations, the observed duration of blooms was much shorter. The phase delay could be explained by the fact that the simulation

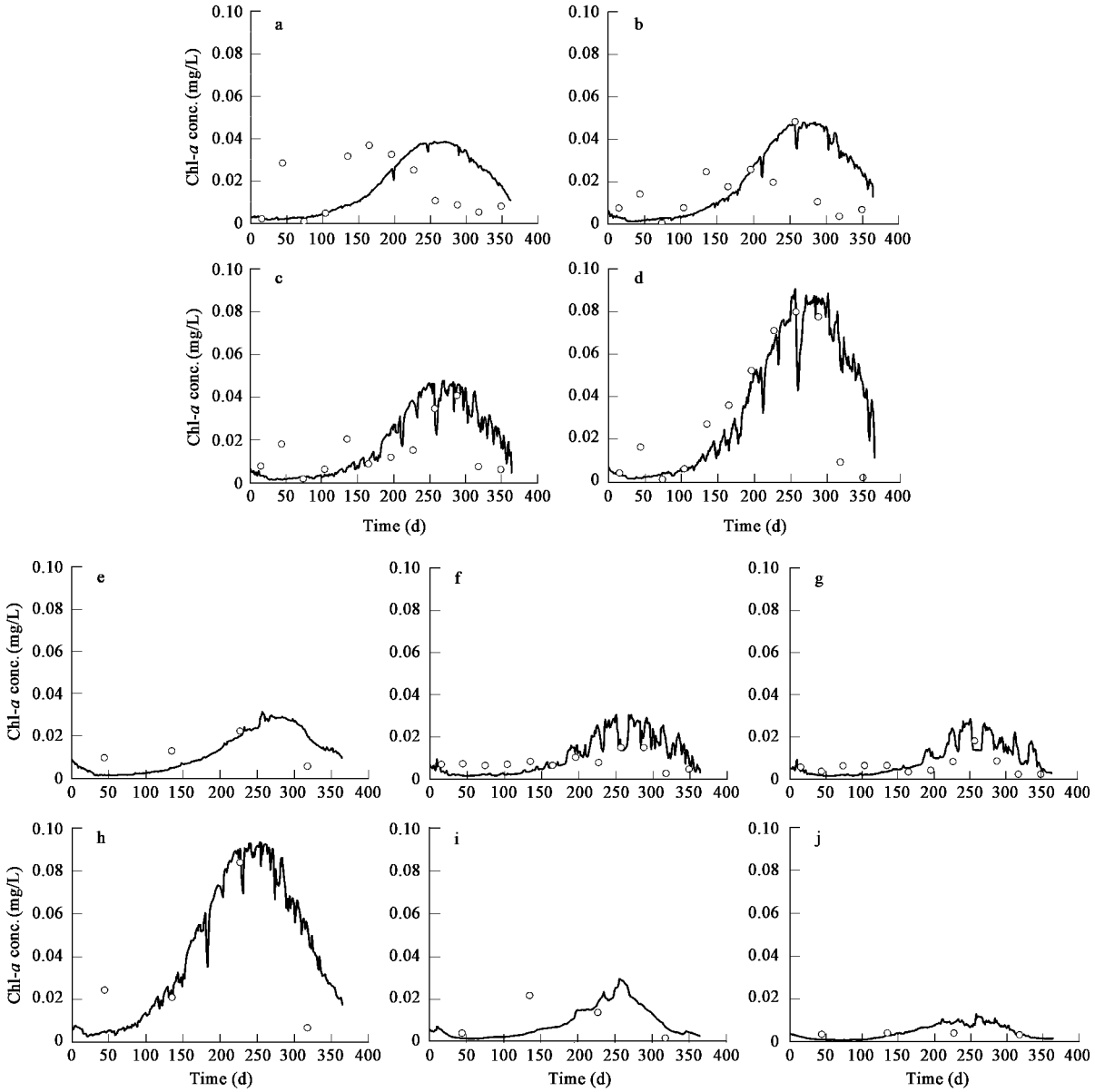

Fig. 4 Modeled (-) and measured (o) chlorophyll-*a* concentrations of stations. (a) Station 1; (b) Station 2; (c) Station 3; (d) Station 4; (e) Station 5; (f) Station 6; (j) Station 7; (h) Station 8; (i) Station 9; (j) Station 10.

was run without considering the complicated boundary conditions, including time-dependent external loads and flow discharge from tributaries.

The modeled result at Station 3, situated at the mouth of Meiliang Bay, was relatively reasonable. The modeled peak value 0.0478 mg/L, appearing at the beginning of October, was only slightly higher than the observed 0.04 mg/L (Fig.4c). Among monitoring stations, the Station 4 was the most eutrophic area. It can be seen from Fig.4d that the model provides a reasonable reproduction of the annual patterns for primary production. Station 5 is located in the semi-closed Gong Bay. In Fig.4e, the fluctuation of chlorophyll-*a* concentration at this station was smooth for both the calculated and observed series, because the hydrodynamic was weak.

Figures.4f and 4g present the algae bloom and collapse patterns at Stations 6 and 7, located at the center of the lake. Comparing these two figures, it is found that the modeled chlorophyll-*a* concentrations are analogous to the observations and the peaks appeared in August simultaneously. At the center of the lake, the maximum observed value was 0.02 mg/L, and the maximum computed value is about 0.025 mg/L.

Station 8 belonging to the west Taihu Lake is close to a heavily polluted tributary, Dapugang River (Fig.3). In early September, the maximum observed chlorophyll-*a* concentration rose to 0.084 mg/L, while the maximum computed value was 0.092 mg/L (Fig.4h). Stations 9 and 10 are located in the east and the south of Taihu Lake where water quality is relatively better. Both modeled results were very close to the observed data (Figs.4i and 4j). The minimum chlorophyll-*a* concentration at Station 9 is lower than 0.01 mg/L.

High primary production is the significant trophic fea-

Table 1 Calibrated values of parameters used in the model

Parameter	Description (Unit)	Value
γ_i	Stoichiometric relation (*i*-different cycle)	–
θ_i	Temperature constant (*i*-different cycle)	1.02–1.08
$Y_{\text{Chl-}a}$	Respiration efficiency of phytoplankton	0.6
Y_{Zp}	Respiration efficiency of zooplankton	0.65
$Y_{\text{ZpChl-}a}$	Predation efficiency factor	0.6
α	Water extinction coefficient (1/m)	0.13
β	Phytoplankton extinction coefficient (1/m per mg/L)	15
I_{s}	Saturation light intensity (MJ/(m^2·d))	12
T_{opt}	Optimum water temperature (°C)	30
$\mu_{\text{Chl-}a}$	Maximum phytoplankton growth rate (1/d)	1.28
$K_{m\text{P}}$	Half saturation constant for phosphorus (mg/L)	0.002
K_{mN}	Half saturation constant for nitrogen (mg/L)	0.025
$k_{d\text{Chl-}a}$	Phytoplankton mortality rate (1/d)	0.27
K_{Zp}	Zooplankton predation rate (1/d)	0.105
$K_{m\text{Zp}}$	Predation half saturation constant (mg/L)	0.06
$K_{d\text{Zp}}$	Zooplankton mortality rate (1/d)	0.12
$\nu_{s\text{Dt}}$	Falling velocity of detritus (m/d)	0.15
$K_{d\text{Dt}}$	Decomposition rate of detritus (1/d)	0.04
K_{dc}	Decomposition rate of DOM (1/d)	0.023
$K_{sr\text{Dt}}$	Floatation rate of sediment (mg/(m^2·d))	20
K_{DOS}	Oxygen consumption rate by sediment (1/d)	0.2
K_{DO}	DO consumption half saturation constant (mg/L)	0.3
$K_{sr\text{Sp}}$	Release rate of phosphorus (mg/(m^2·d))	6.0
$K_{sr\text{Sn}}$	Release rate of nitrogen (mg/(m^2·d))	34
$K_{sr\text{Sc}}$	Release rate of DOM (mg/(m^2·d))	200
K_{sed}	Fraction ration of sediment	0.6

ture of Taihu Lake. Comparing the modeled results of the ten monitoring stations, it can be found that algal blooms mainly occurs in the north lake (Stations 1–5), including Meiliang Bay and Gong Bay. The trophic status in south and east lake (Station 9, 10) is acceptable because of the relatively thin sediment thickness and low pollution loads. The trophic status in central lake (Station 6, 7) is in between. It is also seen that the trophic status is in accord with the sediment thickness, which means that the sediment has a strong influence on eutrophication in this lake. The results of the ten stations have a similar temporal pattern that is characterized by slowly rising in winter and spring, drastically propagating in summer and collapsing in late fall. It is in accordance with the temporal varying of solar and water temperature.

3 Conclusions

The study developed a 3D eutrophication model, which coupled a biochemical module and a hydrodynamics module. The influences of relevant hydrological conditions, external pollution loads, wind, solar radiation, water temperature and sediments release were considered in the model. After sensitivity analysis and calibration, the model was applied to the Taihu Lake. The Comparisons between model results and field data in year 2000 indicated that the model is able to simulate the eutrophication dynamics in Taihu Lake with a reasonable accuracy. In addition, the model improved the capability for simulations of spatial-temporal variations, compared to the previous studies.

From the study, the eutrophication features of Taihu Lake were revealed that: (1) the north Taihu Lake, including Meiliang Bay, Zhushan Bay and Xu Bay, is susceptible to algal blooms with high chlorophyll-*a* concentrations; (2) besides the influence of wind-induced currents, the spatial distribution of sediments is another key factor; (3) algal blooms in Taihu Lake usually take place in summer and early fall with duration of about two months, except for the Meiliang Bay due to the complicated boundary conditions; (4) the temporal variation of chlorophyll-*a* concentration is similar to that of annual solar radiation and water temperature, which indicates that meteorological forcing plays an important role in the eutrophication dynamics.

Acknowledgements

This work was supported by the Hi-Tech Research and Development Program (863) of China (No. 2005AA6010100401) and the National Natural Science Foundation of China (No. 30200030).

References

Chau K W, 2004. A three-dimensional eutrophication modeling in Tolo Harbour. *Applied Mathematical Modelling*, 28(9): 849–861.

Chen Q, Mynett A E, 2003. Integration of data mining techniques and heuristic knowledge in fuzzy logic modelling of eutrophication in Taihu Lake. *Ecological Modelling*, 162: 55–67.

Drago M, Cescon B, Iovenitti L, 2001. A three-dimensional numerical model for eutrophication and pollutant transport. *Ecological Modelling*. 145(1): 17–34.

Drago M, Iovenitti L, 2000. σ-Coordinates hydrodynamic numerical model for coastal and ocean three-dimensional circulation. *Ocean Engineering*, 26: 1065–1085.

Hong X, 2005. Mathematics model building of the water environmental in Taihu Lake and the study of the total discharge quantity control. Master dissertation presented to Hohai University.

Hu W P, Pu P, Qing B Q, 1998. A three-dimensional numerical simulation on the dynamics in Taihu Lake, China (I): the water level and the current during the 9711 typhoon process. *Journal of Lake Science*, 10(4): 17–24.

Hu W P, Qing B Q, 2002. A three-dimensional numerical simulation on the dynamics in Taihu Lake, China (IV): transportation and diffusion of conservative substance. *Journal of Lake Science*, 14(4): 311–316.

Liang R J, Zhong J W, 1994. A three-dimensional numerical simulation of wind-driven water current in Taihu Lake. *Journal of Lake Science*, 6(4): 289–297.

Lonin S A, Tuchkovenko Y S, 2001. Water quality modelling for the ecosystem of the Ciénaga de Tesca coastal lagoon. *Ecological Modelling*, 144(2-3): 279–293.

Mao J Q, 2005. Study on assessment methods and numerical simulation of eutrophication in lakes and reservoirs. PhD dissertation presented to Tsinghua University.

Muhammetoglu A, Soyupak S, 2000. A three-dimensional water quality-macrophyte interaction model for shallow lakes. *Ecological Modelling*, 133: 161–180.

Pang Y, Yao Q, Pu P, 1998. A comprehensive numerical simu- lation and computation on the physics and environment of air water system in Taihu Lake area. Beijing: China Meteorological Press.

Xu Q J, Qing B Q, Chen W M, Chen Y W, Gao G, 2001. Ecological simulation of algae growth in Taihu Lake. *Journal of Lake Science*, 13(2): 149–157.

Zhang J, Jørgensen S E, Mahler H, 2004. Examination of structurally dynamic eutrophication model. *Ecological Modelling*, 173(4): 313–333.

Zhu Y C, Cai Q M, 1998. Studies on three-dimensional hydro-dynamic model in Meiliang Bay of Taihu Lake (II): the diffusion of nutrient salt under the action of three-dimensional currents. *Oceanologia et Limnologia Sinica*, 29(2): 169–173.